Surface segregation energy in bcc Fe-rich Fe-Cr alloys

A. V. Ponomareva,[1] E. I. Isaev,[1] N. V. Skorodumova,[2] Yu. Kh. Vekilov,[1] and I. A. Abrikosov[3]
[1]*Theoretical Physics Department, Moscow Steel and Alloys Institute, Moscow, Russia*
[2]*Department of Physics, Uppsala University, Uppsala, Sweden*
[3]*Department of Physics, Chemistry and Biology (IFM), Linköping University, Linköping, Sweden*
(Received 22 December 2006; revised manuscript received 23 March 2007; published 6 June 2007)

The exact muffin-tin orbitals (EMTO) technique in conjunction with the coherent-potential approximation (CPA) as well as the projector-augmented-wave (PAW) method have been used to calculate the surface segregation energy of Cr at the (100) surface of Fe-rich bcc Fe-Cr alloys. We find that PAW results strongly depend on the supercell size used in the calculations. In particular, for large supercells, the surface segregation energy of Cr is positive, which means that Cr should not segregate toward the surface of diluted alloys. This is in agreement with our EMTO-CPA results as well as previous surface Green's-function calculations. However, the surface segregation energy of Cr is negative if small unit cells are used for simulations. This is in agreement with previous full-potential supercell calculations. We explain such a size dependence by a peculiar concentration dependence of interatomic interactions in ferromagnetic Fe-Cr alloys.

DOI: 10.1103/PhysRevB.75.245406 PACS number(s): 68.35.Dv, 81.05.Bx

I. INTRODUCTION

The bcc Fe-Cr binary system constitutes the basis of ferritic stainless steels known for their excellent corrosion-resistant properties. These properties originate from the formation of a stable surface Cr oxide film, which prevents further oxidation of an alloy deep into the bulk. On the atomic scale, the necessary supply of Cr atoms to the surface should be provided by a segregation of Cr atoms toward the surface. It is, therefore, interesting and important to find the physical mechanism behind the Cr segregation.

The problem here comes from the existing controversy in both experimental data and theoretical results. Suzuki *et al.*[1] using angle-resolved x-ray photoelectron spectroscopy have investigated the effect of Cr segregation in oxide films formed on the surfaces of $Fe_{77}Cr_{13}$ and $Fe_{75}Cr_{25}$ alloys at room temperature. An enrichment of the surfaces with Cr has been observed after *in situ* heating of the samples at 973 K in ultrahigh vacuum.[1] In this case, the effective thickness of the segregated layer was less than 10 Å but the Cr concentration in the film exceeded the bulk Cr content by a factor of 3. Oxide films formed on the segregated surface of the samples exposed to air at room temperature were found to be thinner as compared to those of unsegregated surfaces. Moreover, the effective thickness of oxide films decreased with Cr concentration in the alloy.[1]

On the other hand, in the scanning tunneling microscopy study reported in Ref. 2, a noticeable Cr enrichment of the (100) surface of Fe has been observed only after the deposition of 2–3 Cr monolayers (ML), and for smaller amounts of deposited Cr, only 10–25 at. % of it remained at the surface, indicating that there is a force driving Cr from the surface into the bulk. Similar results have been obtained by Venus and Heinrich[3] in angle-resolved Auger electron spectroscopy studies, where it has been found that almost half a Cr monolayer deposited onto the Fe surface at $T=296$ K migrated into subsurface layers.

According to the theoretical calculations by Nonas *et al.*,[4] done by the full-potential Korringa-Kohn-Rostoker (FP-KKR) method within the local-density approximation (LDA), the segregation energy E_{segr} of Cr at the (100) surface of Fe is −0.05 eV at $T=0$ K. A similar result, −0.03 eV, has been obtained by Geng[5] in the calculations using the all-electron full-potential linearized augmented plane-wave (FLAPW) method. Although the negative value of the surface segregation energy means that Cr atoms should segregate toward the surface, as it has been noticed by Geng,[5] its small absolute value cannot ensure a surface segregation of Cr at high temperatures due to an entropy driven compensation effect.

A quite different result for the surface segregation energy of Cr has been obtained by Ruban *et al.*[6] Using the surface Green's-function technique based on the Korringa-Kohn-Rostoker method, the coherent-potential approximation (CPA), and atomic sphere approximation (ASA), they found quite a large positive value (0.2 eV) for the surface segregation energy of Cr at the (100) surface of bcc Fe. It has been suggested in Ref. 6 that this result could originate from a well-known error of ASA in reproducing the fcc-bcc structural energy difference. The results of earlier theoretical studies are summarized in Table I.

In the present work, we address this controversy by calculating the surface segregation energy of Cr at the (100) surface of bcc Fe by two different methods: the projector-

TABLE I. Summary of previous calculations of the surface segregation energy E_{segr} (in eV) of Cr toward the (100) surface of diluted bcc Fe-Cr alloys.

Method	E_{segr} (eV) GGA	LDA
FP-KKR[a]		−0.05
FLAPW[b]	−0.03	
LMTO-ASA+M[c]		0.2

[a]Reference 4.
[b]Reference 5.
[c]Reference 6.

augmented-wave (PAW) method[7,8] [as implemented in VASP (Ref. 9)] and the exact muffin-tin orbitals (EMTO) method in the coherent-potential approximation (CPA).[10–14] Although in the EMTO method the spherical approximation is used for the shape of one-electron density and potential during self-consistent calculations, the electron states have the correct normalization inside the corresponding Wigner-Seitz cells, which allows us to eliminate the error in the one-electron energy spectrum. Besides the use of the full-charge density technique,[11] following the self-consistent calculations allows one to substantially reduce the ASA error in the electrostatic and exchange-correlation energies, bringing the accuracy of the method to the level of full-potential techniques.

II. DETAILS OF THE CALCULATION

The calculations of total and segregation energies were performed by the PAW method as implemented in the Vienna *ab initio* simulation package[7–9] (VASP) and by the EMTO (Refs. 10 and 11) method. The PAW calculations were performed using both the generalized gradient approximation (GGA) with the Perdew-Wang parametrization[15] and the LDA with the Ceperly-Alder parametrization.[16] For Fe and Cr, the $3d^7 4s^1$ and $3d^5 4s^1$ electrons were treated as valence. The cutoff energy of 850 eV was used. Surface segregation energy was calculated using several supercells: $2\times2\times7$ (28 atoms), $2\times2\times9$ (36 atoms), $2\times2\times11$ (44 atoms), $2\times4\times7$ (56 atoms), $3\times3\times7$ (63 atoms), $3\times3\times9$ (81 atoms), and $3\times3\times9$ (99 atoms). To avoid any interaction between the slabs, they were separated by 20 Å of vacuum. The $8\times8\times1$ and $6\times6\times1$ k-point grids were used for the $2\times2\times N$ (N is the number of layers in the slab) and $3\times3\times N$ supercells, respectively. For the $2\times4\times7$ supercell the grid of $8\times6\times1$ k points was employed.

To estimate the segregation energies (E_{segr}) in the supercell technique, we calculated the energies for the supercells where one Fe, either in the topmost surface layer ($E_{\mathrm{Cr},surf}$) or in the middle of the slab ($E_{\mathrm{Cr},bulk}$), was substituted with a Cr atom. We used the following definition of E_{segr}:

$$E_{segr} = E_{\mathrm{Cr},surf} - E_{\mathrm{Cr},bulk}, \tag{1}$$

where $E_{\mathrm{Cr},surf(bulk)}$ is the total energy of the supercell with a Cr atom in the surface (bulk) layer. The total energies were converged within the accuracy of 10^{-3} eV/cell. All the supercells were fully relaxed, and the atomic positions were optimized until the forces acting on atoms became smaller than 10^{-3} eV/Å. Atomic relaxations were studied in detail in the PAW-GGA calculations since LDA underestimates the equilibrium lattice spacing by 8%.

To consider the diluted limit, we used the EMTO method combined with the coherent-potential approximation[10–14] for the electronic structure calculations of slabs of random Fe-Cr alloys. A slab geometry was again used in the surface segregation energy calculations by the EMTO-CPA method; however, instead of using a single Cr impurity as in the case of the PAW calculations, we considered a single layer of a random $Fe_{1-c}Cr_c$ alloy placed either at the surface or in the middle of the slab. Then, the surface segregation energy was obtained as follows:

$$E_{segr} = \frac{dE^{rand}_{surf}}{dc_s} - \frac{dE^{rand}_{bulk}}{dc_b}, \tag{2}$$

where $E^{rand}_{surf(bulk)}$ are the total energies of a slab with a random alloy either in the surface layer or in the bulk. The concentration derivatives in Eq. (2) were calculated by using three different compositions with the concentration step of 1 at. %.

In the EMTO calculations, we used three different slabs: 12-layer (seven atomic and five vacuum layers), and 18-layer (13 atomic and five vacuum layers), and 18-layer (18 atomic layers without vacuum) slabs. The Brillouin-zone (BZ) integration was performed using 91 k points in the irreducible two-dimensional BZ for supercells with vacuum layers and using 225 k points in the calculations of the bulk total energies. The energy integration was carried out in the complex plane on a semielliptic contour comprising 20 energy points. The s, p, d, and f muffin-tin orbitals were included into the basis set.

It is known that in some cases, GGA provides a better description of the bulk ground-state properties of $3d$ metals than LDA. At the same time, the ability of GGA to correctly reproduce surface properties has recently been questioned.[17] Therefore, in our PAW calculations, we employed both LDA (Ref. 16) and GGA (Ref. 15) comparing the results obtained using the two approximations. In the EMTO-CPA calculations, we did not optimize the lattice geometry and carried out only LDA calculations using the Vosko-Wilk-Nusair parametrization[18] of the exchange-correlation energy. In fact, we did not observe any strong dependence of the segregation energy on the used approximation when the calculations were performed for the same lattice parameter. We carried out two series of calculations using both the experimental (2.86 Å) and theoretically calculated (2.83 Å) lattice parameters. The latter appeared to be very similar in the GGA-PAW and LDA-EMTO calculations.

III. RESULTS

The segregation energies calculated by the EMTO-CPA and PAW methods are presented in Table II. E_{segr} is positive for all the considered supercells except the relaxed and unrelaxed $2\times2\times7$ slabs and the relaxed $2\times4\times7$ slab, which exhibit negative segregation energies. These results demonstrate that the calculated E_{segr} depend on the size of the supercell used in the calculations. Notice that E_{segr} calculated for the relaxed $2\times4\times7$ supercell is in good agreement with the results by Geng[5] (see Table I), where the same supercell was used in the all-electron FLAPW calculations. Moreover, E_{segr} calculated for large supercells by the PAW and EMTO-CPA methods are found to be in good agreement with each other.

Let us first discuss the structural and magnetic properties of the relaxed surface slabs obtained by the PAW method and the influence of surface relaxation on segregation energies and local magnetic moments. Surface relaxation was calculated for all the studied slabs following the recipe of Ref. 19. Changes in the position of surface and subsurface layers due to relaxation are found to be small irrespective of the supercell size (Fig. 1). The surface layer of Fe exhibits 0.2% in-

TABLE II. Surface segregation energy of Cr toward the (100) surface of bcc Fe calculated by the EMTO-CPA and PAW methods. The star (⋆) indicates E_{segr} for which (dE_{bulk}/dc) in Eq. (2) was calculated using slabs without vacuum layers, i.e., vacuum layers were replaced by Fe layers.

	EMTO E_{segr} (eV)			
	a=2.83 Å		a=2.86 Å	
Slab	LDA	GGA	LDA	GGA
7 layers	0.180		0.23	
13 layers	0.185		0.26	
13 layers (⋆)	0.130		0.20	

	PAW E_{segr} (eV)				
	a=2.83 Å			a=2.86 Å	
		GGA			
Cell	LDA	Unrelaxed	Relaxed	LDA	GGA
2×2×7		−0.009	−0.043		
2×4×7		0.03	−0.02		
3×3×7		0.05	−0.009		
2×2×9	0.110	0.103	0.080		
3×3×9	0.130	0.135	0.090	0.19	0.209
2×2×11		0.08	0.069		
3×3×11		0.093	0.064		

ward relaxation. On the contrary, surface Cr atoms are shifted toward vacuum by about 0.25%. The subsurface layer shows the outward relaxation of 1% (Fig. 1). Surface relaxation slightly reduces the segregation energies (Table II). The reduction of E_{segr} due to relaxation becomes less significant as the supercell size increases.

Magnetic moments calculated using both the EMTO-CPA and PAW methods are presented in Table III. At low Cr concentrations, the magnetic moments of the Cr atoms both at the (100) surface and in the bulk are parallel to each other and antiparallel to the magnetic moments of the Fe atoms. The calculated magnetic moment for a Cr atom on the (100) Fe surface is about 3.2 μ_B (LDA), in agreement with the result of *in situ* magnetometer measurements (3.0 μ_B) for the first Cr monolayer on Fe(100).[20] Our results indicate that magnetic moments are rather insensitive to surface relaxation. Indeed, the changes in the magnetic moments of the surface Fe and Cr atoms due to relaxation are only about 0.05 μ_B. Importantly, our slab EMTO-CPA calculations (as well as the PAW calculations for the large supercells) reveal a correlation between E_{segr} and the magnetic moment of Cr: the Cr segregation energies are lower for the slabs with lower Cr magnetic moments (compare Tables II and III).

We also simulated an elemental segregation step calculating the segregation energy of Cr atoms from bulk into the surface (s), subsurface ($s-1$), and second subsurface ($s-2$) layers for the random $Fe_{95}Cr_{05}$ alloy. Calculations were performed for the 18-layer slab at the experimental lattice parameter a=2.86 Å. The results of these calculations are presented in Table IV. Note that Cr segregation into the subsurface layer is even less energetically favorable compared to that in the surface layer, and dE_{s-2}/dc is not yet equal to the value calculated for the slab center. Therefore, the second subsurface layer still "feels" the presence of the surface.

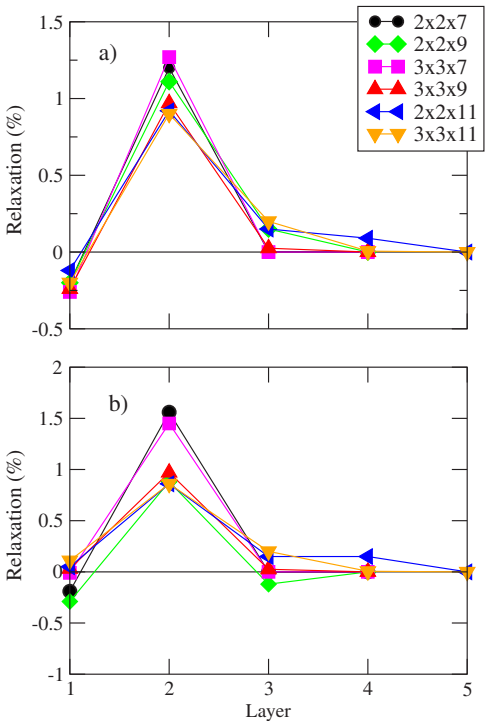

FIG. 1. (Color online) Changes in the interlayer distances of atomic layers with respect to their ideal positions (see Ref. 19) calculated for the supercells of different sizes simulating (100) surface of bcc Fe: (a) without and (b) with one Cr impurity.

TABLE III. Magnetic moments of the Cr and Fe atoms calculated by means of the EMTO-CPA and PAW methods. LDA and GGA exchange-correlation potentials and experimental (2.86 Å) lattice parameters were used for these calculations. The star (⋆) indicates calculations using slabs without vacuum layers, and diamond (◇) refers to the random $Fe_{95}Cr_{05}$ alloy. Magnetic moments shown in numerator and denominator stand for Cr and Fe, respectively.

	Cr in a bulk position (Cr/Fe) (μ_B)		Cr in a surface position (Cr/Fe) (μ_B)	
Cell, method	LDA	GGA	LDA	GGA
(3×3×9), PAW	−1.76/2.2	−2.1/2.38	−3.2/2.90	−3.37/2.92
13 layers, EMTO	−1.77/2.2		−3.21/2.99	
13 layers (⋆), EMTO	−1.73/2.2			
13 layers (◇), EMTO	−1.66/2.2		−3.20/2.95	

TABLE IV. The segregation energy (E_{segr}) of the Cr atoms in the surface (s), subsurface ($s-1$), and second subsurface ($s-2$) layers of the random $Fe_{95}Cr_{05}$ alloy.

Layer	E_{segr} (eV)
s	0.12
$s-1$	0.27
$s-2$	0.07

IV. ORIGIN OF THE SIZE EFFECT

A. Cluster expansion of the total energy

A relatively strong dependence of E_{segr} on the size of the supercell observed in the PAW calculations suggests that it originates from the strong concentration dependence of the interatomic interactions in bcc Fe-rich Fe-Cr alloys. Such a dependence has previously been found in the generalized perturbation method[21,22] (GPM) calculations of the first several effective pair interactions by Hennion[23] and then experimentally confirmed in the neutron-diffraction experiments by Mirebeau *et al.*[24] It can also be seen in the enthalpy of formation of the Fe-Cr alloys in the ferromagnetic state[25,26] as an abrupt change of its sign near 10 at. % Cr.

In order to analyze effective interactions in Fe-Cr system, the total energy E_{tot} was mapped onto the effective Ising-like Hamiltonian,

$$E_{tot} = V^{(0)} + \sum \left[V^{(1)}\langle\sigma\rangle + \sum_s V^{(2,s)}\langle\sigma_i\sigma_j\rangle^s + \cdots \right], \quad (3)$$

where i, j are lattice sites and σ_i^s denote spin variables, taking values of +1 or −1 depending on the type of the atom occupying site i. The average products of the spin variables, $\langle\sigma_i\sigma_j\cdots\sigma_k\rangle$, are the multisite correlation functions which form the complete basis for the total-energy expansion,[27] $V^{(0)}$ is the reference energy, which, in fact, is the total energy of a random equiatomic alloy, and $V^{(d,s)}$ is the effective cluster interaction, which corresponds to the cluster of the order d and type s. For instance, $V^{(2,1)}$, $V^{(2,2)}$, and $V^{(2,3)}$ are the effective pair interactions in the first, second, and third coordination shells, respectively. The on-site interaction $V^{(1)}$, which is the effective chemical potential, can be neglected in the canonical ensemble calculations. In the case of inhomogeneous systems, Eq. (3) should be written as

$$E_{tot}^{surf} = V^{(0)} + \sum_\lambda \left[V_\lambda^{(1)}\langle\sigma_\lambda\rangle + \sum_{\lambda',s} V_{\lambda\lambda'}^{(2,s)}\langle\sigma_{\lambda;i}\sigma_{\lambda';j}\rangle^s + \cdots \right], \quad (4)$$

where the effective interactions $V_{\lambda\lambda'\lambda''\ldots}^{(d,s)}$ now depend on the cluster order d and its type s as well as on the relative position of the cluster $\lambda\lambda'\cdots$, which designates those atoms of the cluster that are located in layers λ, λ', λ'', and so on.[28] The on-site interactions $V_\lambda^{(1)}$ in this case can be obtained by differentiation of E_{tot}^{surf} of an equiatomic alloy surface with respect to a layer concentration Ref. 29:

$$V_\lambda^{(1)} = \left.\frac{dE_{tot}^{surf}}{d\langle\sigma_\lambda\rangle}\right|_{\langle\sigma_\lambda\rangle=0} - \left.\frac{dE_{tot}^{surf}}{d\langle\sigma_{\lambda_b}\rangle}\right|_{\langle\sigma_{\lambda_b}\rangle=0}, \quad (5)$$

where λ_b designates a layer in bulk, or in practice, the center layer of a slab. Expression (5) is similar to the definition of the segregation energy, but on-site potentials $V_\lambda^{(1)}$ are calculated for the equiatomic alloy in order to single out contributions to an on-site potential from higher-order interactions. In Eq. (5), the volume is chosen equal to the equilibrium volume for a given alloy concentration. The pair potentials $V_{\lambda\lambda'}^{(2,s)}$ have been calculated using the GPM method.[21,22] Importantly, the formalism presented in Ref. 27 is developed for concentration independent interactions, while GPM effective potentials are concentration dependent. However, there is a simple relationship between concentration dependent and independent interactions, in which the dependence on concentration for a given interaction is given through concentration independent interactions of higher orders.[30]

B. Interatomic interactions and size effect

The on-site surface potentials (V_s^1) are similar for the 7- (−1828 K) and 13-layer (−2050 K) slabs. The negative sign of V_s^1 means that it is more favorable to have Fe atoms at the (100) surface [$\sigma_i=1$ corresponds to an Fe atom and $\sigma_i=-1$ corresponds to a Cr atom, in Eq. (4)]. Besides, positive values of the pair potentials characterize a trend to ordering while negative ones indicate a tendency to clustering.

Let us first discuss the results obtained for small supercells, $2\times2\times7$ and $2\times4\times7$ in our PAW calculations. We note that in these supercells, the in-layer Cr concentration is rather high, 25% and 12.5%, respectively. Our EMTO-CPA calculations show that the pair interactions between the nearest ($V_b^{2,1}$) and next-nearest ($V_b^{2,2}$) neighbors obtained for the Fe slabs where the middle layer had 25% of Cr (Fig. 2) are different from the potentials calculated for the diluted bulk alloys (see inset in Fig. 2). This difference is most pronounced for $V_b^{2,1}$. Thus, effective interactions in Fe-Cr alloys depend strongly on concentration.

The concentration dependence of the nearest-neighbor and next-nearest-neighbor pair potentials at the surface appears to be much weaker than that in bulk (see inset in Fig. 2). Consequently, the pair interactions at the surface obtained for different in-plane Cr concentrations are in much better agreement with each other. Thus, the calculations of the segregation energy carried out for small supercells with large in-plane concentrations of the Cr atoms can strongly overestimate the tendency toward phase separation in the bulk. As a matter of fact, such structures contain a highly unstable pseudo-ordered Fe-Cr middle layer that leads to an enhancement of the last terms in Eqs. (1) and (2). At the same time, the first term in these equations is relatively well described in the calculations done for small supercells.

An increase of the supercell size in the x and y dimensions corresponds to a decrease of the in-plane Cr concentration. According to Fig. 2, $V_b^{2,1}$ (filled triangles for 5% Cr) and $V_b^{2,2}$ (filled circles for 5% Cr) calculated for larger cells are in much better agreement with the values obtained in bulk cal-

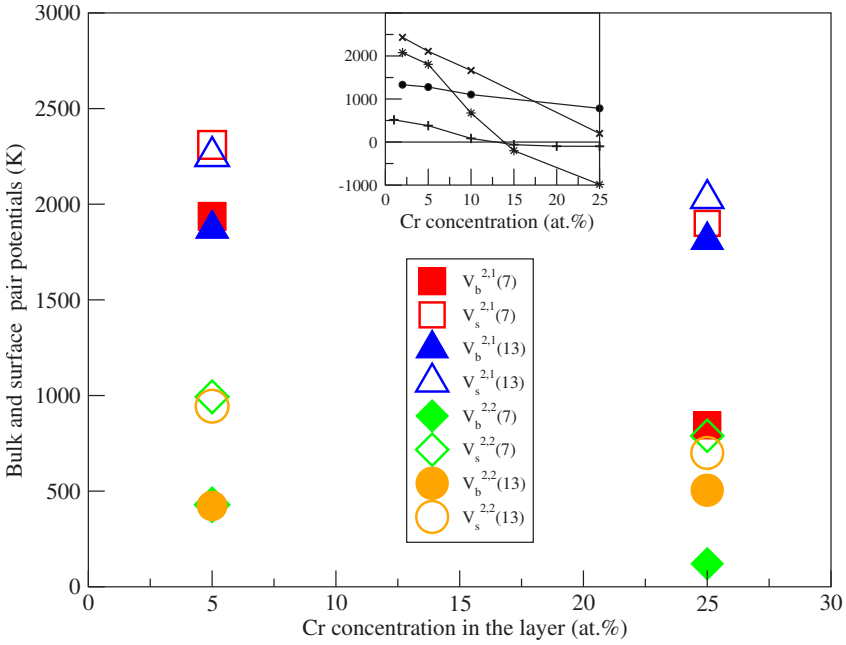

FIG. 2. (Color online) The nearest-neighbor $V_b^{2,1}$ and next-nearest-neighbor $V_b^{2,2}$ pair potentials in the bulk (filled symbols) and $V_s^{2,1}$, $V_s^{2,2}$ for the (100) surface (open symbols) of Fe-Cr alloys calculated by EMTO-CPA technique using the 7-layer and 13-layer Fe slabs with 5 and 25 at. % of Cr in the middle or in the surface layers. The concentration dependence of pair potentials $V_b^{2,1}$ (∗), $V_b^{2,2}$ (+) for diluted bulk alloys and concentration dependence of surface pair potentials $V_s^{2,1}$ (×), $V_s^{2,2}$ (●) calculated by the EMTO-CPA method using the 13-layer random $Fe_{1-x}Cr_x$ alloy slabs are shown in the inset.

culations for very diluted alloys. Generally, these values are more positive than those for smaller cells, indicating an enhanced stability of bulk alloys at low Cr concentration, which, in its own turn, makes surface segregation unfavorable energetically.

This analysis indicates that the in-plane Cr concentration is very important and it should be small enough if one wants to calculate segregation energies accurately. Of course, an increase of the supercell size in the z direction should also improve the accuracy of the calculations even for supercells with relatively high in-plane concentration of Cr. Indeed, as evident from Fig. 2, $V_b^{2,1}$ (filled triangles) and $V_b^{2,2}$ (filled circles) calculated for the 13-layer slab ($c_{in\text{-}plane}^{Cr}=25\%$) are in much better agreement with the corresponding values obtained in the diluted limit.

Let us state it again: To have a good estimate of a segregation energy, it is very important to monitor the in-plane Cr concentration rather than just total Cr concentration and to avoid nearly ordered in-plane structures.

Another observation following from Table II is that the segregation energies calculated by the PAW method are somewhat lower than the corresponding EMTO values even for the largest supercell used in the PAW calculations. This trend can be understood if one takes into account the concentration dependence of the bulk mixing enthalpy ΔH calculated by Olsson *et al.*[25] using both EMTO and PAW methods. ΔH for ferromagnetic bcc Fe-Cr alloys turn out to be negative for the alloys with low Cr concentrations and positive for those with higher Cr content. The mixing enthalpy exhibits a minimum according to both methods, but its depth and width obtained in the EMTO-CPA and PAW calculations are different. This results in different values for the bulk chemical potential in the diluted limit. The PAW mixing enthalpies are higher as compared to those from EMTO-CPA. According to the PAW calculations, it is less favorable to dissolve Cr in Fe bulk. This, in turn, might lead to less positive E_{segr}.

Unfortunately, to the best of our knowledge, the experimental values of the mixing enthalpy for ferromagnetic Fe-Cr bcc alloys are not available. However, the authors of Ref. 25 pointed out that the theoretically estimated concentration (EMTO method) at which the mixing enthalpy changes its sign is in fair agreement with the concentration for which the change of short-range order parameters from ordering to clustering type has been observed in experiments.

C. Magnetism and exchange interactions

Further, we discuss the influence of magnetism on the segregation phenomena in Fe-Cr alloys. We performed the fixed spin moment[31] bulk calculations using the EMTO-CPA method, which showed that pair interactions $V_b^{2,i}$ became stronger as the absolute value of the magnetic moment on Cr atoms increased. This indicates that the Cr atoms with larger absolute values of magnetic moments bind stronger to the Fe atoms and, in this case, it is more difficult to move a Cr atom from bulk to the surface that corresponds to the increase of the segregation energy.

Although the segregation energy of Cr atoms at the (100) surface of diluted Fe-Cr alloys obtained in our calculations is positive, meaning that the Cr atoms favor bulk rather than surface positions, there are reasons to believe that in Cr steels, a surface segregation of Cr does occur ensuring a high corrosion resistance of these materials. One possible reason for such a segregation could be the oxygen-chromium interaction, which attracts Cr atoms from the bulk to the surface suppressing small positive values of the Cr segregation energy. However, even in the absence of oxygen, Cr segregation is possible in nondiluted alloys. Indeed, as we mentioned above, in alloys with higher Cr concentration, the repulsion between the Cr atoms is reduced, and a clustering process can start. Magnetic interactions between the Cr atoms result in an antiferromagnetic (AFM) ordering in clusters composed of the Cr atoms. Recently, Klaver *et al.*[32] have

observed this effect in their total-energy calculations for different arrangements of Cr impurities in bcc Fe. Here, we analyze it by calculating the so-called magnetic exchange interaction parameters, J_2 of the Heisenberg Hamiltonian,[33] in the framework of the magnetic force theorem and the EMTO-CPA method.

Our calculations show that in the surface layer of the $Fe_{95}Cr_{05}$ alloy, the values of J_2 for Fe-Cr and Cr-Cr nearest-neighbor interactions are equal to −2.02 and −3.19 mRy, respectively, while they are −1.56 and −1.14 mRy for the corresponding bulk alloy. Cr atoms try to avoid forming pairs because, in this case, they cannot have the AFM alignment of their magnetic moments with respect to each other as well as to surrounding Fe atoms. As the concentration of Cr increases, it becomes unavoidable to have Cr pairs. The magnetic structure of such alloys becomes frustrated and this favors a tendency toward clustering in the bulk.[32] However, as a matter of fact, another possibility for Cr atoms to avoid magnetic frustrations is to segregate toward the surface. Our calculations show that placing 2 Cr ML onto the Fe(100) surface allows the moments of the Cr atoms to be AFM ordered with respect to each other as well as to those of the first Fe layer. Interestingly, the thickness of the segregated layer deduced from experiments was about 10 Å, i.e., a few atomic layers.[1]

On the other hand, the Cr layers of a submonolayer thickness deposited onto the (100) surface of pure Fe demonstrate low stability.[3] In particular, it has been shown that only 25% of Cr from the 0.4 Cr ML originally deposited onto the Fe(100) substrate could actually be found at the surface. After the deposition of 0.4–1 Cr ML, about 10% could be found in the surface layer. The surface becomes enriched with Cr only when the thickness of the deposited films exceeded 2–3 Cr ML.

These results can be understood based on the moment ordering considerations discussed above. Indeed, in the Cr films with thicknesses less than 1 ML, magnetic frustration cannot be avoided. In this case, either the moments of the Cr atoms within the layer must be ordered ferromagnetically or some of the surface Cr atoms should have moments parallel to those of the Fe atoms, or the latter should be ordered antiferromagnetically with respect to each other, or the magnetic structure must be noncollinear. As we mentioned above in the diluted bulk Fe-Cr alloys, the repulsion between Cr atoms is stronger in the surface layer than in the bulk that can make Cr leave the surface for the bulk.

In summary, the analysis of the experimentally observed behavior of submonolayer thick Cr films on the Fe(100) surface suggests that there is no Cr segregation in the diluted Fe-Cr alloys. This is in agreement with the results of our calculations. However, the segregation might take place in the case of Fe-Cr alloys with a higher Cr concentration as a result of an interplay between magnetic and chemical interactions.

V. CONCLUSION

Using the EMTO-CPA and PAW methods, we have calculated the segregation energy of Cr atoms at the (100) surface of bcc Fe-Cr alloys in the diluted limit. The results of our studies allow us to draw the following conclusions:

(i) The segregation energy obtained in the supercell PAW calculations strongly depends on the supercell size.

(ii) This dependence is explained by a significant concentration dependence of the effective pair interactions between atoms in the bulk material. The effect is much weaker at the (100) surface than it is in the bulk.

(iii) For large supercells, the PAW and EMTO-CPA results are in good agreement with each other, and we find a positive segregation energy, meaning that Cr atoms favor bulk rather than surface positions.

(iv) The conclusions above are supported by the analysis of the known experimental observations.

ACKNOWLEDGMENTS

Critical discussions with A. V. Ruban are gratefully acknowledged. Financial support from the Swedish Foundation for Strategic Research (SSF) and the Swedish Research Council (VR) are acknowledged. We are grateful to the Royal Swedish Academy of Sciences (KVA) for supporting the collaboration between Russian and Swedish scientists. A.V.P., E.I.I., and Yu.Kh.V. thank RFBR (Grants No. 04-02-16823 and No. 05-02-17461) and NWO (Grant No. 047.016.005) for financial support. Most of the calculations were performed at the Joint Supercomputer Center, Moscow, Russia, and at the National Supercomputer Center, Linköping, Sweden.

[1] S. Suzuki, T. Kosaka, H. Inoue, M. Isshiki, and Y. Waseda, Appl. Surf. Sci. **103**, 495 (1996).
[2] A. Davies, J. A. Stroscio, D. T. Pierce, and R. J. Celotta, Phys. Rev. Lett. **76**, 4175 (1996).
[3] D. Venus and B. Heinrich, Phys. Rev. B **53**, R1733 (1996).
[4] B. Nonas, K. Wildberger, R. Zeller, and P. H. Dederichs, Phys. Rev. Lett. **80**, 4574 (1998).
[5] W. T. Geng, Phys. Rev. B **68**, 233402 (2003).
[6] A. V. Ruban, H. L. Skriver, and J. K. Norskov, Phys. Rev. B **59**, 15990 (1999).
[7] G. Kresse and D. Joubert, Phys. Rev. B **59**, 1758 (1999).
[8] P. E. Blöchl, Phys. Rev. B **50**, 17953 (1994).
[9] G. Kresse and J. Furthmüller, Comput. Mater. Sci. **6**, 15 (1996); Phys. Rev. B **54**, 11169 (1996).
[10] L. Vitos, H. L. Skriver, B. Johansson, and J. Kollar, Comput. Mater. Sci. **18**, 24 (2000).
[11] L. Vitos, Phys. Rev. B **64**, 014107 (2001).
[12] L. Vitos, I. A. Abrikosov, and B. Johansson, Phys. Rev. Lett. **87**, 156401 (2001).
[13] B. L. Györffy, Phys. Rev. B **5**, 2382 (1972).
[14] J. S. Faulkner, Prog. Mater. Sci. **27**, 1 (1982).
[15] J. P. Perdew and Y. Wang, Phys. Rev. B **45**, 13244 (1992).

[16] D. M. Ceperley and B. J. Alder, Phys. Rev. Lett. **45**, 566 (1980).
[17] A. Bogicevic, S. Ovesson, P. Hyldgaard, B. I. Lundqvist, H. Brune, and D. R. Jennison, Phys. Rev. Lett. **85**, 1910 (2000); A. E. Mattsson and D. R. Jennison, Surf. Sci. **520**, L611 (2002).
[18] S. H. Vosko, L. Wilk, and M. Nusair, Can. J. Phys. **58**, 1200 (1980).
[19] N. V. Skorodumova, K. Hermansson, and B. Johansson, Phys. Rev. B **72**, 125414 (2001).
[20] C. Turtur and G. Bayreuther, Phys. Rev. Lett. **72**, 1557 (1994).
[21] F. Ducastelle, *Order and Phase Stability in Alloys* (North-Holland, Amsterdam, 1991); J. P. Perdew, *Electronic Structure of Solids* (Akademie, Berlin, 1991).
[22] A. V. Ruban, S. Shallcross, S. I. Simak, and H. L. Skriver, Phys. Rev. B **70**, 125115 (2004).
[23] M. Hennior, J. Phys. F: Met. Phys. **13**, 2351 (1983).
[24] I. Mirebeau, M. Hennior, and G. Parette, Phys. Rev. Lett. **53**, 687 (1984).
[25] P. Olsson, I. A. Abrikosov, and J. Wallenius, Phys. Rev. B **73**, 104416 (2006).
[26] P. Olsson, I. A. Abrikosov, L. Vitos, and J. Wallenius, J. Nucl. Mater. **321**, 84 (2003).
[27] J. M. Sanchez, F. Ducastelle, and D. Gratias, Physica A **128**, 334 (1984); J. M. Sanchez and D. de Fontane, *Structure and Bonding in Crystals* (Academic, New York, 1981), p. 117.
[28] A. V. Ruban, I. A. Abrikosov, D. Ya. Kats, D. Gorelikov, K. W. Jacobsen, and H. L. Skriver, Phys. Rev. B **49**, 11383 (1994).
[29] L. V. Pourovskii, A. V. Ruban, I. A. Abrikosov, Yu. Kh. Vekilov, and B. Johansson, Phys. Rev. B **64**, 035421 (2001).
[30] W. Schweika and A. E. Carlsson, Phys. Rev. B **40**, 4990 (1989).
[31] E. I. Isaev, L. V. Pourovskii, A. M. N. Niklasson, Yu. Kh. Vekilov, B. Johansson, and I. A. Abrikosov, Phys. Rev. B **65**, 024435 (2002).
[32] T. P. C. Klaver, R. Drautz, and M. W. Finnis, Phys. Rev. B **74**, 094435 (2006).
[33] A. I. Liechtenstein, M. I. Katsnelson, and V. A. Gubanov, J. Phys. F: Met. Phys. **14**, L125 (1984); Solid State Commun. **54**, 327 (1985); A. I. Liechtenstein, M. I. Katsnelson, V. P. Antropov, and V. Gubanov, J. Magn. Magn. Mater. **67**, 65 (1987).